



Contents lists available at ScienceDirect

Thin Solid Films

journal homepage: www.elsevier.com/locate/tsf

Luminescent coatings prepared from optimized YAG:Ce nanoparticles

G. Dantelle ^{*}, M. Salaün, R. Bruyère, S. Kodjikian, A. Ibanez

Univ. Grenoble Alpes, Inst. NEEL, F-38042 Grenoble, France
CNRS, Inst. NEEL, F-38042 Grenoble, France

ARTICLE INFO

Article history:

Received 9 February 2017

Received in revised form 25 April 2017

Accepted 1 May 2017

Available online xxxx

Keywords:

Phosphors

YAG:Ce

Nanocrystals

Spray-deposition

Films

ABSTRACT

$\text{Y}_3\text{Al}_5\text{O}_{12}$ nanoparticles doped with Ce^{3+} ions (YAG:Ce) were prepared by solvothermal synthesis. For short reaction times, very small YAG:Ce grains are formed and aggregate together with a preferred orientation, as proved by X-ray diffraction analysis and transmission electron microscopy. For longer reaction times, individual well-crystallized and faceted YAG:Ce nanoparticles are observed. The growth of the nanoparticles under solvothermal conditions seems to be driven by self-oriented aggregation and coalescence leading to single-crystals at the nanoscale. For larger YAG:Ce nanoparticles (18 ± 5 nm), the internal luminescence quantum yield is measured to be $27 \pm 5\%$ and seems only limited by surface defects or species, regarding the high crystalline quality of the nanocrystals. Such nanocrystals are deposited onto glass substrates by spray-deposition, a simple deposition technique which allows the formation of binder-free films. Micron-thick translucent films, exclusively composed of stacked YAG:Ce nanoparticles, are formed, while the particle morphology and optical properties are not modified by the deposition process.

© 2017 Elsevier B.V. All rights reserved.

1. Introduction

The yttrium aluminum garnet, $\text{Y}_3\text{Al}_5\text{O}_{12}$, matrix doped with Ce^{3+} (YAG:Ce) is a well-known phosphor extensively used in white light emitting diodes (wLEDs). YAG:Ce micro-crystals present strong advantages such as well-controlled syntheses, a perfect chemical stability, high luminescence quantum yields (above 85%) and a good photostability, explaining its commercial use [1,2]. However, the present design of wLEDs, consisting in placing micrometer-sized YAG:Ce crystals encapsulated inside epoxy domes above InGaN blue-LEDs, is not entirely satisfactory. The main drawbacks are: (1) the use of epoxy or silicone resins, which present bad ageing properties leading to a degradation of the lighting properties of wLEDs, especially at high power, and (2) the use of micro-crystals, which induces strong scattering effects, resulting in a limited external efficiency (typically around 65%) [3,4,5].

To overcome these drawbacks, different strategies are explored to develop resin-free YAG:Ce coatings and/or films with controlled scattering rate. Among the different works, Potdevin et al. developed efficient luminescent YAG:Tb³⁺ films based on sol-gel chemistry, which offer the advantage to spread out homogeneous films using simple techniques (dip-coating, spin-coating) [6]. This process requires an annealing step after deposition, inducing uncontrolled cracks inside the films and thus, a difficulty to master their scattering rate. A more recent work

proposes to use transparent YAG:Ce ceramic films obtained by solid-state reaction under vacuum, which appears as a very promising technology though more costly [7]. Another strategy consists in a two-step process, involving first the development of efficient YAG:Ce nanoparticles and second, their shaping in a binder-free film. This strategy offers the possibility of optimizing the structure and the optical properties of the nanophosphors independently of the film preparation.

The preparation of YAG:Ce nanoparticles, using a solvothermal method, has been reported 20 years ago [8]. This synthesis method leads to the formation of pure YAG:Ce nanocrystals; however they present a polycrystalline morphology and consequently a porosity, which is responsible for low internal luminescent quantum yields (iQY) and for the photo-oxidation of Ce^{3+} into non luminescent Ce^{4+} [9]. Some strategies exist to improve of the iQY. For instance, Revaux et al. annealed YAG:Ce nanoparticles previously dispersed into silica at 1000 °C and succeeded in increasing the iQY by a factor of 2. However, the process is highly time-consuming [10]. Hussain et al. reported an iQY increase by grafting Au nanoparticles onto the YAG nanoparticle surface through plasmonic effects [11], but this process adds another step in the elaboration of phosphors and increases significantly their cost.

In this paper, we show the possibility of obtaining well-crystallized and monodisperse YAG:Ce nanoparticles by controlling the synthesis conditions. Then, these nanocrystals were deposited onto a glass substrate through a spray-deposition technique. Such a technique allows the formation of micron-thick nanoparticle-based films without the use of any binder and opens the possibility of controlling the film scattering rate by filling its open porosity with media of various refractive

^{*} Corresponding author.

E-mail address: geraldine.dantelle@neel.cnrs.fr (G. Dantelle).

index [12]. Our whole study is performed on YAG doped with 1 mol% Ce^{3+} , i.e. a low doping concentration, which ensures no concentration quenching.

2. Experimental section

2.1. YAG:Ce nanoparticle synthesis

The synthesis of $\text{Y}_{2.97}\text{Ce}_{0.03}\text{Al}_5\text{O}_{12}$ nanoparticles is adapted from [9]. Briefly, aluminum isopropoxide, yttrium acetate and cerium acetate were weighted in stoichiometric proportions and mixed in 1,4-butanediol. In order to favor homogeneous nucleation and obtain monodisperse particles, the precursor concentration was kept low. Typically, 12.5 mmol of Al isopropoxide were dispersed in 141 mL of butanediol. The mixture was placed into a 200 mL autoclave (Autoclave Engineers), equipped with a manometer, which was then purged with Ar for a few minutes to remove air and thus prevent Ce oxidation during the reaction. The autoclave was heated at 300 °C within 1 h (ramp of 300 °C/h) and remained, under stirring, at this temperature for different times, ranging from 30 min to 24 h. The final pressure inside the autoclave depends on the reaction time as shown on Fig. 1. This evolution, linear at short reaction times and constant for longer times, indicates that the pressure inside the autoclave is auto-generated by both precursor decompositions and partial phase change of the solvent. The steady-state conditions occur after a reaction time of around 500 min. After the dwell at 300 °C (referred to as reaction time in the following), the temperature was decreased to room temperature at a speed of 100 °C/h. After the reaction, the resulting solutions were washed twice with ethanol and centrifugation. The typical YAG:Ce particle concentration was 10 g/L in ethanol. For some analysis, powder samples were required. They were obtained by drying the alcoholic solution at 110 °C for 30 min.

2.2. YAG:Ce nanoparticle-based film elaboration

Luminescent films were prepared from the different concentrated solutions of YAG:Ce nanoparticles in ethanol (10 g/L). To obtain the best performances in terms of film luminescence, the samples with optimized YAG:Ce nanocrystals were preferred. The selected coating technique was the spray deposition, which consists in creating a mist of nanoparticles from the colloidal solution of YAG:Ce dispersed in ethanol through an air flux (pneumatic spray) [13,14]. The particles were deposited onto microscope slides previously heated at 120 °C to favor a rapid drying and avoid the formation of droplets at the substrate surface.

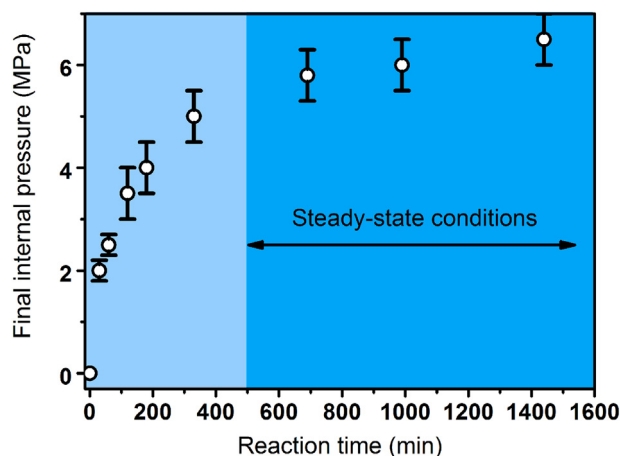


Fig. 1. Evolution of the final pressure inside the autoclave as a function of reaction time. For reactions shorter than 500 min, the autogenous pressure built up inside the autoclave; whereas for longer reactions, the pressure remains constant (~60 bars) leading to steady-state reactions.

Indeed, such droplets would induce particle leaking and associated film inhomogeneities.

2.3. YAG:Ce nanoparticle characterizations

X-ray powder diffraction (XRD) patterns of YAG:Ce were collected with the θ -2 θ geometry, under ambient conditions using a Siemens D8 Advance diffractometer ($\lambda_{\text{Cu}} = 1.54056 \text{ \AA}$, 40 mA, 40 kV) in the 2 θ range 10–60°, with a step size of 0.01° and an acquisition time of 3.5 s/step. XRD patterns were analyzed through the LeBail method to determine phase purity, cell parameters, crystallite size and internal strains [15].

On the other hand, all the samples were characterized by Transmission Electron Microscopy (TEM, Philips CM300) performed at 300 kV. The sample preparation consisted in evaporating droplets of nanoparticles dispersed in ethanol onto carbon grids.

The photoluminescence (PL) of YAG:Ce nanoparticle solutions was studied using a Safas Xenius spectrofluorometer, under ambient conditions. In order to avoid any bias due to scattering effect, diluted solutions (with a typically concentration of 20 mg/L) were used. Emission spectra were recorded under a 457 nm excitation, whereas excitation spectra were recorded for an emission wavelength of 565 nm. In addition, iQYs were measured for the different nanopowders using a 4-mm integrating sphere (covered by Spectralon polymer) under 457 nm excitation wavelength and for the emission range between 500 and 700 nm.

2.4. YAG:Ce nanoparticle-based film characterizations

The film structure was analyzed by XRD using a Siemens D8 diffractometer in a θ -2 θ configuration ($\lambda_{\text{Cu}} = 1.54056 \text{ \AA}$, 40 mA, 40 kV). Films were characterized by Scanning Electron Microscopy (SEM, Zeiss Ultra Plus, operating at 3 kV). Images were taken from the top of the film, as well as from the edge to evaluate the thickness and porosity. Their PL was also recorded using the Safas Xenius spectrofluorometer.

3. Results and discussion

3.1. Control of the particle size

YAG:Ce nanoparticles obtained for different reaction times were characterized by XRD. Fig. 2a shows the LeBail fit to the diffraction pattern of the powder obtained after 24 h and is representative of the XRD data. The good fit indicates that the peaks are well indexed with the $I\bar{a}3d$ space group. Only a small peak at $2\theta = 49.8^\circ$ is not indexed. It could correspond to the presence of a boehmite phase in very small quantity. For all reaction times (Fig. 2b), similar results were obtained.

The LeBail fit gives the full width at half maximum (FWHM) of all diffraction peaks, allowing the calculation of the crystallite size through the Scherrer formula, considering the whole diffraction pattern. The evolution as a function of reaction time is shown on Fig. 3a. The longer the synthesis the larger the crystallite size, indicating a favored growth mechanism for longer reaction times.

A deeper analysis was performed by the Williamson-Hall (WH) method [16]. This method allows measuring the deformation rate, ϵ , corresponding to the strains within the nanoparticles, according to the following equation [16]:

$$\frac{\text{FWHM}}{\lambda} \cos\theta = \frac{1}{L_c} + \epsilon \frac{\sin\theta}{\lambda} \quad (1)$$

The WH analysis is shown on Fig. 3b for four different samples, while the corresponding results are gathered on Table 1. At short reaction times, the values of the crystallite size obtained by WH analysis are larger than the ones obtained by Scherrer analysis, indicating the diffraction peaks are broadened by other phenomena than the finite size of the crystalline domains. The WH analysis indicates the presence of internal

Download English Version:

<https://daneshyari.com/en/article/8033334>

Download Persian Version:

<https://daneshyari.com/article/8033334>

[Daneshyari.com](https://daneshyari.com)